SUPPORTING INFORMATION

Opening Magnesium Storage Capability of Two-Dimensional MXene by Intercalation of Cationic Surfactant

Min Xu,[Δ†,‡] Shulai Lei,[Δ†] Jing Qi,[‡] Qingyun Dou,[†,¶] Lingyang Liu,[†,¶] Yulan Lu,[‡] Qing Huang,[†,§] Siqi Shi,[†,∥] and Xingbin Yan[*†]

[†]Laboratory of Clean Energy Chemistry and Materials, State Key Laboratory of Solid Lubrication, Lanzhou Institute of Chemical Physics, Chinese Academy of Sciences, Lanzhou 730000, P. R. China

[‡]School of Physical Science and Technology, Lanzhou University, Lanzhou 730000, China

[¶]University of Chinese Academy of Sciences, Beijing 100039, P.R. China

[§]Division of Functional Materials and Nano-Devices, Ningbo Institute of Material Technology and Engineering, Chinese Academy of Science, Ningbo 315201, P.R. China

[∥]School of Materials Science and Engineering, Shanghai University, Shanghai 200444, P.R. China

[Δ] Contributed equally to this work

* The corresponding author. E-mail: xbyan@licp.cas.cn

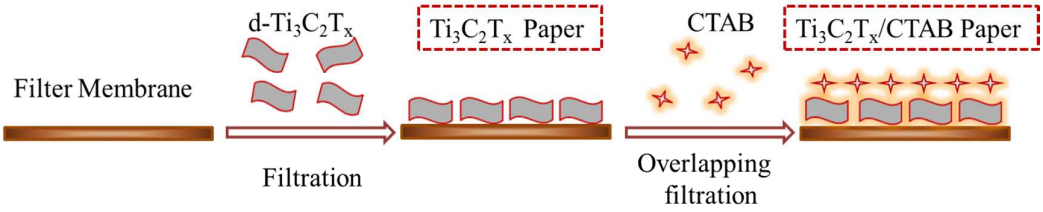

Figure S1 The formation process of freestanding $Ti_3C_2T_x$ and $Ti_3C_2T_x$/CTAB papers by vacuum filtration method.

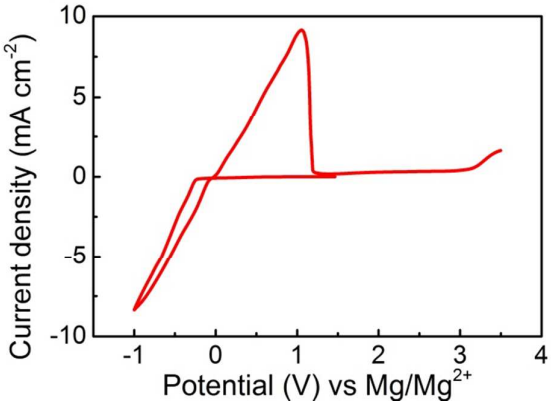

Figure S2. Typical CV curve (at a scan rate of 5 mV s^{-1}) of 0.4 M $(PhMgCl)_2$-$AlCl_3$/THF (APC) electrolyte using a platinum foil as the working electrode, two freshly polished magnesium ribbons as the reference and counter electrodes. The APC electrolyte was prepared by following the steps of the literature (*Advanced Materials* **2007,** *19*, 4260-4267).

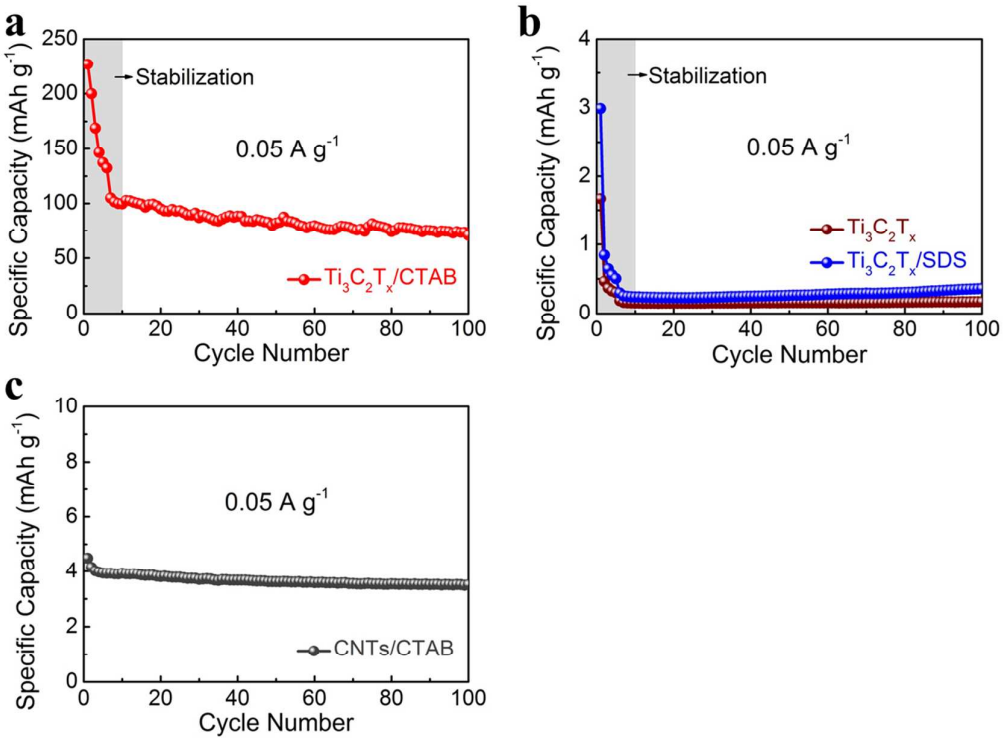

Figure S3. The discharge capacity as a function of cycle number at 0.05 A g^{-1} for (a) $Ti_3C_2T_x$/CTAB electrode, (b) $Ti_3C_2T_x$ and $Ti_3C_2T_x$/SDS electrodes and (c) CNTs/CTAB electrode. The gray parts were the stabilization (first at 0.02 A g^{-1} for 6 cycles and then at 0.05 A g^{-1} for 4 cycles) process.

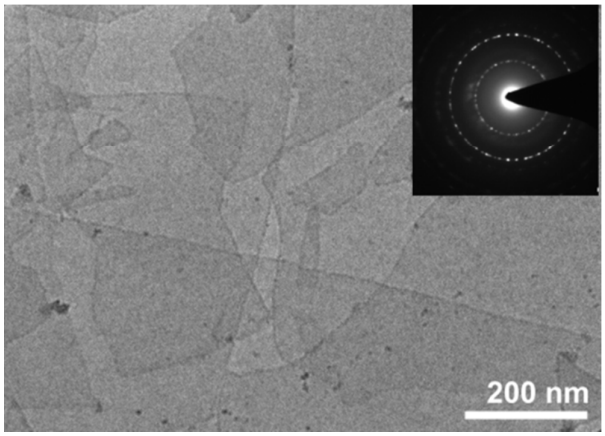

Figure S4. TEM image of $Ti_3C_2T_x$ flakes. Inset shows the selected area electron diffraction pattern.

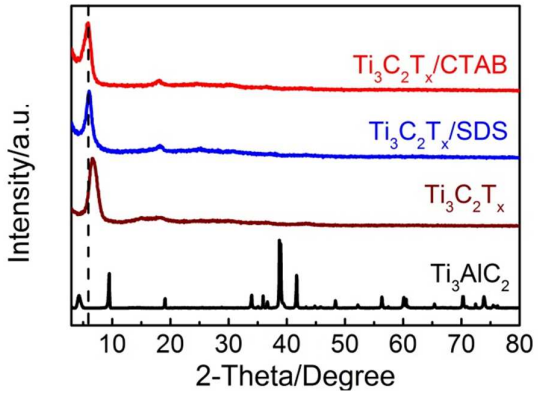

Figure S5. XRD patterns of powdery Ti_3AlC_2, paper-like $Ti_3C_2T_x$, $Ti_3C_2T_x$/SDS and $Ti_3C_2T_x$/CTAB samples.

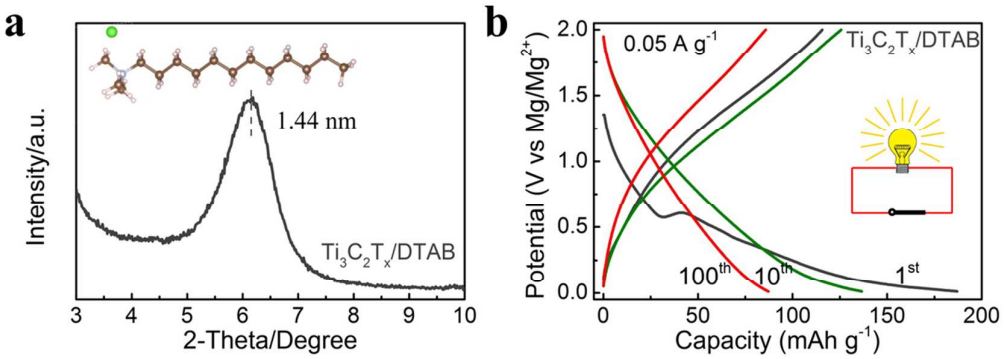

Figure S6 a) XRD pattern of $Ti_3C_2T_x$/DTAB sample. Inset showing the structure schematic of DTAB. b) GCD curves of $Ti_3C_2T_x$/DTAB electrode at the 1st (gray lines), the 10th (green lines) and the 100th (red lines) cycles at 0.05 A g^{-1}.

Figure S7 Digital image of a water drop on paper-like $Ti_3C_2T_x$ (a), $Ti_3C_2T_x$/SDS (b) and $Ti_3C_2T_x$/CTAB (c). The contact angles were measured to be 58°, 65° and 62°, respectively.

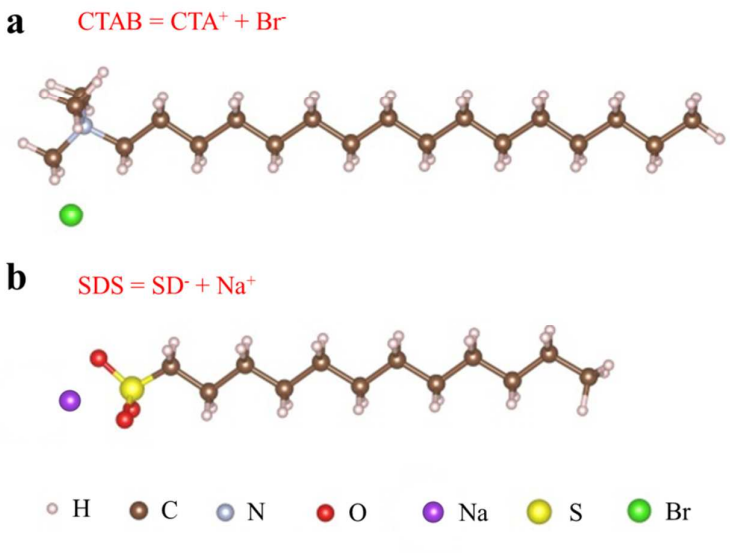

Figure S8. Structural schematics of CTAB (a) and SDS (b).

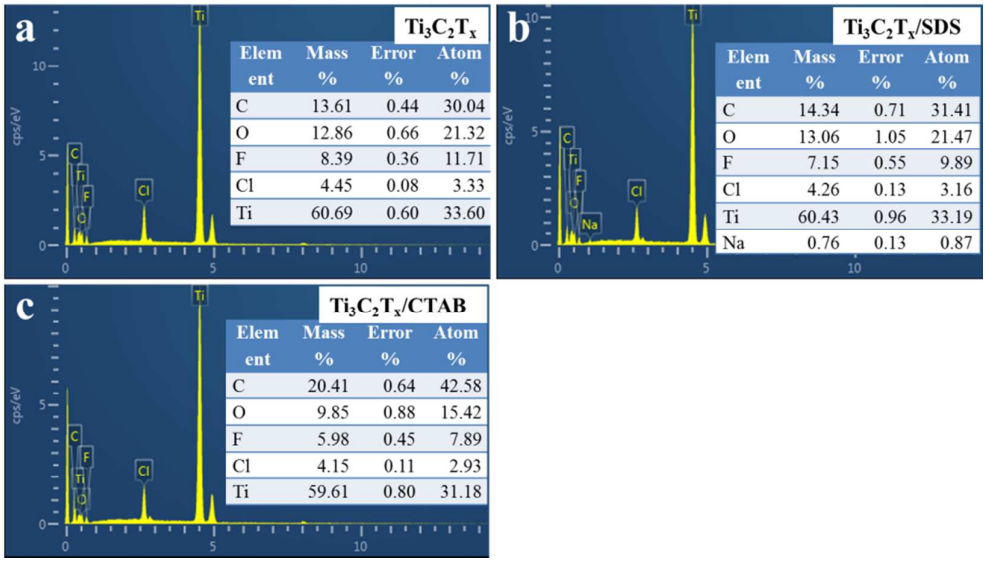

Figure S9. Energy-dispersive spectroscopies of paper-like $Ti_3C_2T_x$ (a), $Ti_3C_2T_x$/SDS (b) and $Ti_3C_2T_x$/CTAB (c).

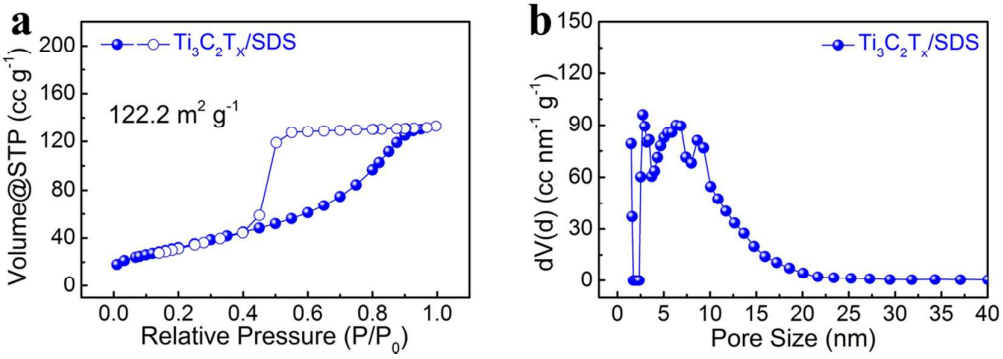

Figure S10. a) N_2 adsorption-desorption isotherms and b) pore size distribution curve of $Ti_3C_2T_x$/SDS paper.

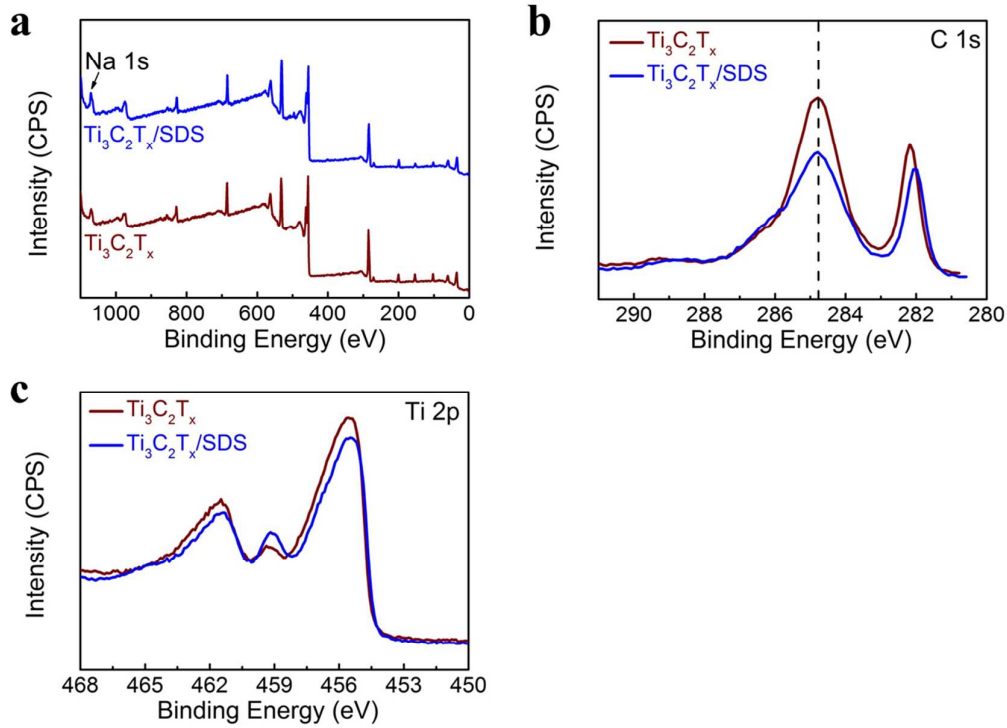

Figure S11. XPS spectra of $Ti_3C_2T_x$ and $Ti_3C_2T_x$/SDS papers: a) full survey spectra, b) C 1s spectra, c) Ti 2p spectra.

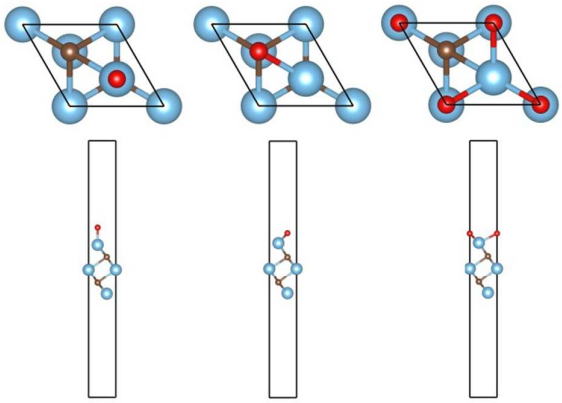

Figure S12. Top-view and side-view of O atom adsorbed on Ti_3C_2 surface at top-site (left), bcc-site (middle) and fcc-site (right).

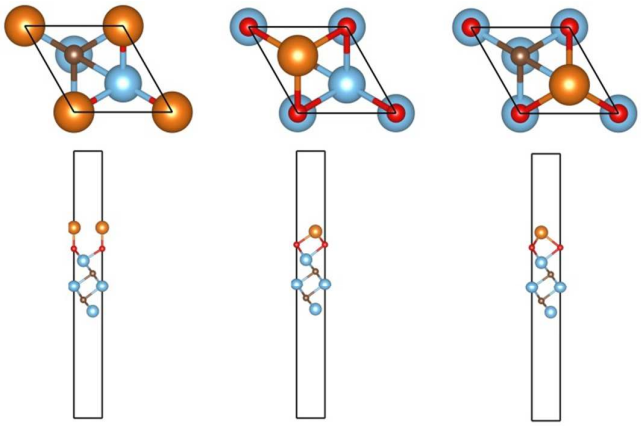

Figure S13. Top-view and side-view of Mg atom adsorbed on Ti_3C_2O surface at top-site (left), fcc-site (middle) and bcc-site (right).

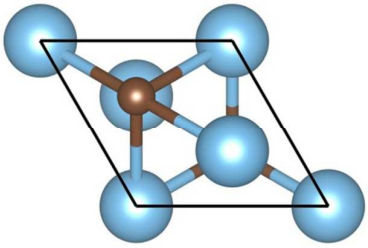

Figure S14. Top-view of Ti_3C_2 crystal structure.

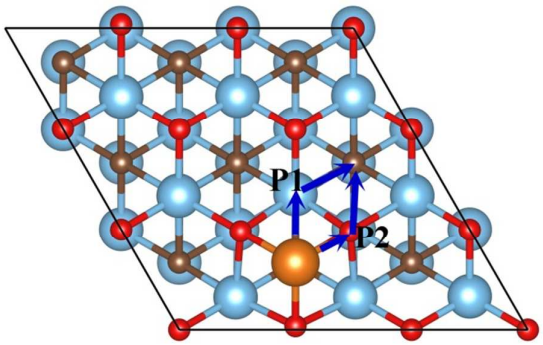

Figure S15. Diffusion paths of Mg^{2+} on Ti_3C_2 surface. As labelled in blue arrows, Mg^{2+} has two diffusion paths, *i.e.,* P1 via top-site of Ti atom and P2 via top-site of O atom. Our theoretical results showed that P2 changed to P1 after NEB calculations.

Table S1. Adsorption energies (in eV) of O atom adsorbed on Ti_3C_2 surface and Mg atom adsorbed on Ti_3C_2O.

Adsorption sites	top	bcc	fcc
$E_{ads}(O/Ti_3C_2)$	-5.41	7.45	-8.16
$E_{ads}(Mg/ Ti_3C_2O)$	-2.39	-2.31	-2.63

Table S2. Bader charger analysis for Mg^{2+} and CTA^+ on Ti_3C_2O surface. Mg was charged positively, 1.64 electron, in Ti_3C_2O/Mg^{2+} system and CTA^+ was charged positively, 1.04 electron, in Ti_3C_2O / Mg^{2+} system, which agree well with experiments. After intercalated CTA^+, *i.e.,* in $Ti_3C_2O/ CTA^+/ Mg^{2+}$ system, bader charge of Mg^{2+} and CTA^+ reduced to 1.38 and 0.81 electron, respectively.

	Ti_3C_2O	CTA^+	Mg^{2+}
Ti_3C_2O / Mg^{2+}	-1.64		1.64
Ti_3C_2O / CTA^+	-1.04	1.04	
$Ti_3C_2O/ CTA^+/ Mg^{2+}$	-2.19	0.81	1.38

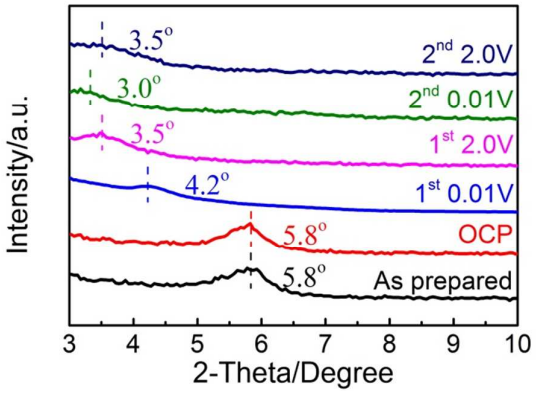

Figure S16. XRD patterns of $Ti_3C_2T_x$/CTAB electrode at different GCD states.

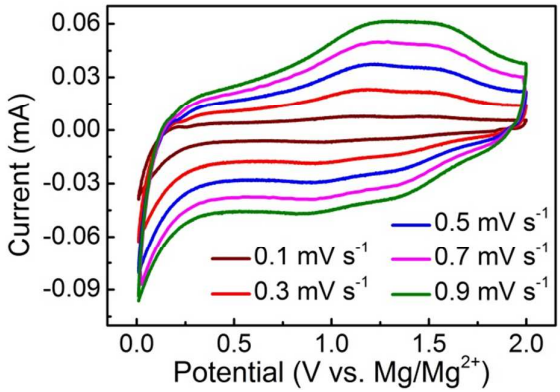

Figure S17. CV curves of the Mg battery using $Ti_3C_2T_x$/CTAB cathode at different scan rates from 0.1 to 0.9 mV s^{-1}.

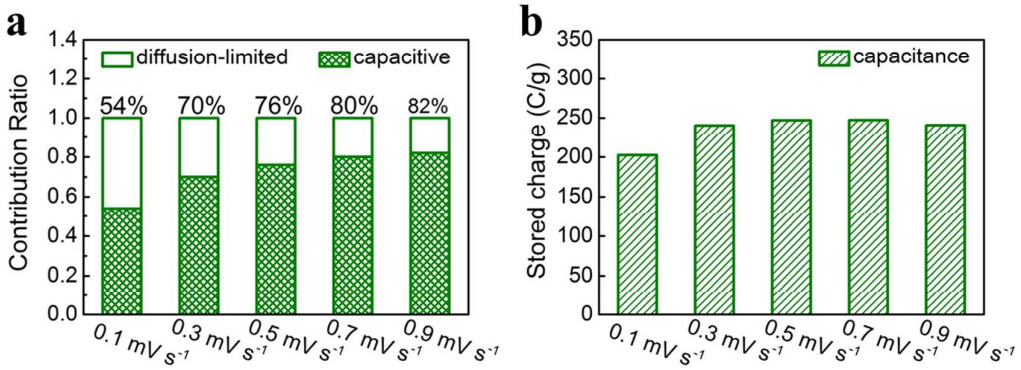

Figure S18. a) Separation of the capacitive and diffusion-limited currents. b) Corresponding dependence of the stored charge by capacitive contribution as a function of the scan rate.

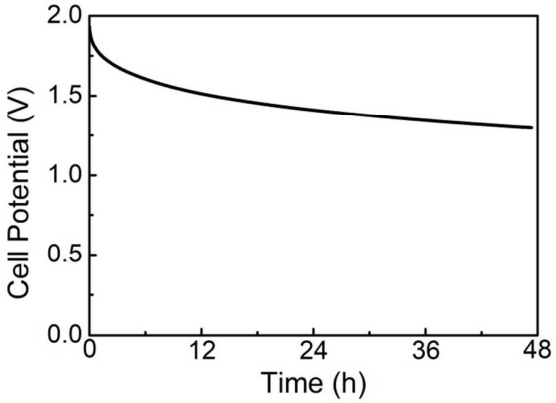

Figure S19. Decay of open circuit potential of the Mg battery using $Ti_3C_2T_x$/CTAB cathode.